6th International Conference on Advances in Experimental Structural Engineering
11th International Workshop on Advanced Smart Materials and Smart Structures Technology
August 1-2, 2015, University of Illinois, Urbana-Champaign, United States

Simple Estimation of Bicycle Lane Condition by Using the Dynamic Response of a Bicycle

Takahiro Yamaguchi[1], Tomonori Nagayama[2], Di Su[3]

1 *Graduate Student, Dept. of Civil Engineering, University of Tokyo, Japan*
E-mail: tyamaguchi@bridge.t.u-tokyo.ac.jp
2 *Associate Professor, Dept. of Civil Engineering, University of Tokyo, Japan*
E-mail: nagayama@bridge.t.u-tokyo.ac.jp
3 *Assistant Professor, Dept. of Civil Engineering, University of Tokyo, Japan*
E-mail: su@bridge.t.u-tokyo.ac.jp

ABSTRACT
While the importance of bicycle transportation is increasing, there is no measurement means to evaluate bicycle lane surface roughness easily and inexpensively with acceptable accuracy. In this paper, a smartphone based system was developed to estimate road profile by measuring vertical vibration acceleration of a city cycle. Firstly, vertical vibration acceleration of commonly used city cycle was examined to clarify factors influencing the acceleration responses. Tire, smartphone fixer, and road profile are shown to affect bicycle vibration characteristics. At 10 km/h, frequency components from 0 to 3 cycle/m reflect road roughness and are not affected by tire or smartphone fixer vibrations. Next, an algorithm to eliminate low frequency noise and transform smartphone acceleration to front or rear tire displacement is proposed. After smartphone displacement is calculated by double integration of acceleration, a correction function theoretically derived from relationship between the tire and the smartphone position is applied. The road profile is estimated as the vertical displacement of the tire. Finally, a field experiment showed that the estimation error of road profile is about 16 % in terms of the maximum values.

KEYWORDS: *Road Profile Estimation, City Cycle, Vibration Characteristics, Road Pavement Roughness*

1. INTRODUCTION

The importance of bicycle transportation is increasing. The number of bicycle registered in Tokyo is steadily increasing these 10 years [1]. According to the increased demand for bicycle transportation, the total length of bicycle lanes rapidly grew by 24 % in 10 years (Figure 1.1) [2]. Furthermore, Tokyo Metropolitan Government plans to double the total length of bicycle lanes by Tokyo Olympic in 2020 [1].

Though the demand for maintenance of bicycle lane pavement condition is also expected to increase, there is no measurement means to evaluate bicycle lane surface condition easily and inexpensively with acceptable accuracy. Maintenance of road surface condition is usually conducted by visual inspection. Visual inspection evaluation is subjective and difficult to guarantee the accuracy. Other methods such as handcart-type road profiler (e.g. DAM [3], Figure 1.2) are relatively expensive and not practical for long distance bicycle lane evaluation.

There is some research about estimating the road conditions by bicycle and motorcycle. Kobana et al. developed a smartphone based system to detect steps and judge step types [4]. However, the system cannot quantify step displacement and detect small (2~3 mm) steps. Oshima et al. examined vertical vibration characteristics of motorcycle and estimate International Roughness Index (IRI) by using measured vertical vibration acceleration [5]. However, vibration characteristics of motorcycle is expected to be different from bicycle and IRI does not indicate local road surface condition such as pot holes and cracks.

In this paper, a smartphone based system was developed to estimate road profile by measuring the vertical vibration acceleration of a city cycle. The measurement system consists of only a smartphone and a cyclometer; measurement can easily and cheaply be executed. In the paper, first vibration acceleration characteristics was examined. Then, the algorithm to calculate road profile was proposed. Finally, the accuracy of the proposed method was confirmed by an experiment in a bicycle lane.

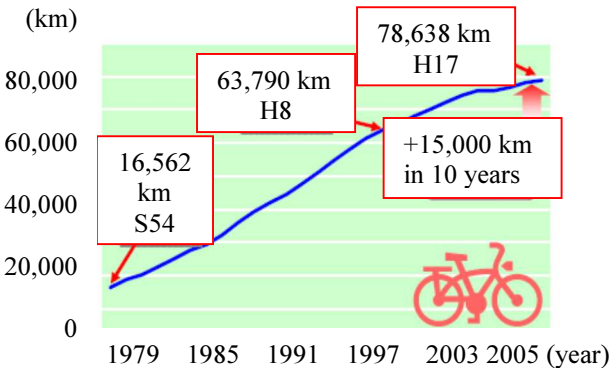

Figure 1.1 Total extension of bicycle lane [2]

Figure 1.2 DAM

2. MEASUREMENT SYSTEM

2.1. Components of measurement system

The measurement system consists of only a bicycle, a smartphone and a cyclometer (Figure 2.1 and 2.2). The bicycle is a 27 inch city cycle. Tri-axial acceleration is measured by the accelerometer of the smartphone, which is fixed on the holder upon the handle. The smartphone is the fifth generation iPod touch installed with iOS 8.1.2. Accelerometer sampling rate is 100 Hz. Data logger application was developed by the Bridge and Structure Laboratory at the University of Tokyo and JIP Techno Science [6]. The application records the tri-axial acceleration at 100 Hz as well as angular velocity and other quantities. As the sampling rate is not accurate, the record is resampled offline based on the time stamp. The smartphone holder is a standard size smartphone holder. The speed of the bicycle is measured by the cyclometer (GARMIN Edge510J), which counts the rear tire rotations using a magnet chip attached to the tire spoke. The sampling rate is 1 Hz. GPS record is also obtained for reference [7].

2.2. Measurement procedure

To synchronize the smartphone and the cyclometer, the data recording of the devices is manually started at the same time. Start points are set 5 to 10 m before objective courses so that the ride speed reaches target constant speeds at the courses. To mark the start point and finish point, the experimenter lightly taps the smartphone holder at the point.

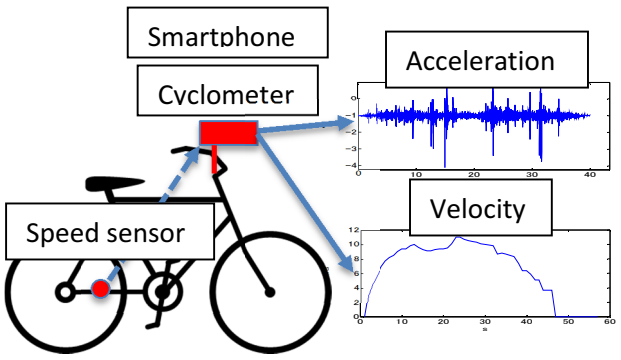

Figure 2.1 Measurement system

Figure 2.2 Smartphone and cyclometer

3. VIBRATION CHARACTERISTICS OF BICYCLE

The vibration characteristics of bicycle is experimentally investigated herein. Free vibration test of a bicycle is first conducted and the vibration characterization during bicycle ride follows.

3.1. Free vibration characteristics of bicycle

Bicycle vibration acceleration is not affected only by road path, but also by other parameters such as bicycle structure and smartphone holder vibration characteristics. Bicycle structure and smartphone holder have their own natural frequencies. These frequencies are estimated by free fall experiment of the front or rear tire and tapping test of the smartphone holder.

Figure 3.1 shows the time history of vertical acceleration when the front tire is dropped. To obtain a free vibration response of the bicycle, data right after the first impact as indicated by the red frame is extracted. Figure 3.2 is the power spectrums of the response when 1) the front tire is dropped with the experimenter on the saddle 2) the front tire is dropped without the experimenter on the saddle 3) the rear tire is dropped with the experimenter on the saddle and 4) the rear tire is dropped without the experimenter on the saddle. In all of these conditions, there are highest peaks at around 14 Hz and small components in the range from 20 to 30 Hz, which are considered to be the vibration components of the bicycle system.

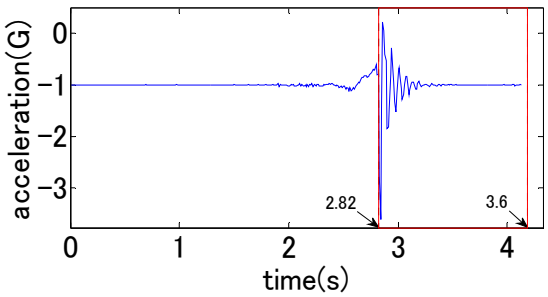

Figure 3.1 Vertical acceleration time history

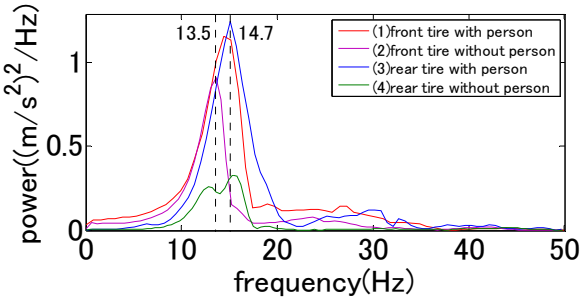

Figure 3.2 Power spectrums of vertical accelerations during free-fall tests

Figure 3.3 is the power spectrum of the vertical acceleration when the side of the smartphone holder, which is fixed on the handle, is tapped by a finger. The natural frequency of smartphone holder is around 40 Hz. Figure 3.4 shows the power spectrums of the vertical acceleration during a drive test where another smartphone is fixed to the handle by packaging tape. The two power spectrums are similar in the 0 to 30 Hz range, and almost the same in the 0 to 10 Hz range. The smartphone holder acceleration is slightly larger above 40 Hz, corresponding to the natural frequency of the smartphone holder.

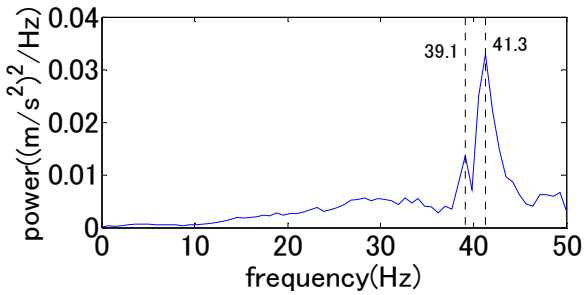

Figure 3.3 Power spectrum of vertical acceleration during tapping tests

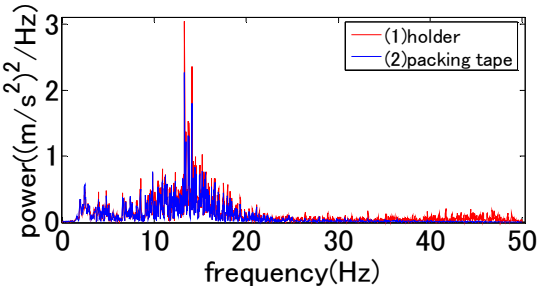

Figure 3.4 Power spectrums of vertical accelerations of two smartphones with different fixtures

3.2. Ride distance estimation

To estimate road profile, which is not influenced by measurement conditions, the running distance needs to be calculated accurately. The speed of bicycle *v(t)* is obtained from the cyclometer. By linear interpolation, the sampling rate of the cyclometer data is changed from 1 Hz to 100 Hz. Distance *x(t)* is calculated by the trapezoidal integration formula as stated in Eq. 3.1. The distance calculated in this manner is confirmed to have an error of about 20 to 30 cm for a 100 m course. This error is much smaller than distance estimation based on GPS data, which has an error of about 2 to 3 m. Therefore, the distance is calculated based on the cyclometer data.

$$x(t) = \frac{v(t)-v(t-dt)}{2} * dt \tag{3.1}$$

Hereafter, the frequency is discussed in terms of spatial cyclic frequency (i.e. cycle/m) instead of temporal cyclic frequency (i.e. Hz). For example, 1 Hz corresponds to 0.36 cycle/m at 10 km/h. The natural frequencies of the bicycle structure and the smartphone holder are 5 cycle/m (14 Hz) and 14.4 cycle/m (40 Hz) respectively.

3.3. Vibration characteristics during bicycle ride

Vibration characteristics during bicycle ride are influenced by the ride speed, tire pressure, and driving path. These influences are examined herein.

Figure 3.5 shows the power spectrums at various speeds from 8 to 12 km/h. The magnitudes of the spectrums increase when the speed increases. A theoretical relationship between bicycle speed v, which is the temporal derivative of distance x, and measured vertical acceleration a, which is the second temporal derivative of road profile h is derived as stated in Eq. 3.2 when the bicycle is assumed to be a rigid body. Eq. 3.3 is a speed calibration formula used in acceleration spectrum comparison. After this calibration, the spectrums below 3 cycle/m match well as in Figure 3.6. Above 3 cycle/m, the spectrums do not match well; the dynamic effect of the bicycle structure is considered large in this high frequency range.

$$a = \frac{d^2h}{dt^2} = \frac{d^2h}{dx^2}\frac{dx}{dt}\frac{dx}{dt} = v^2\frac{d^2h}{dx^2} \tag{3.2}$$

$$a_2 = \frac{{v_2}^2}{{v_1}^2}a_1 \tag{3.3}$$

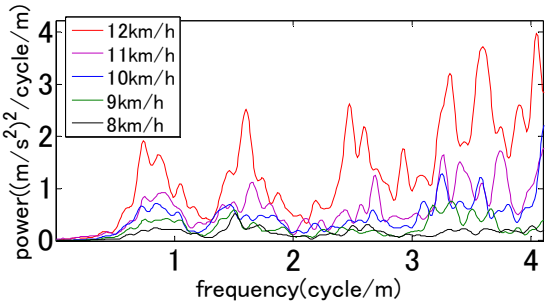

Figure 3.5 Power spectrums at different speed

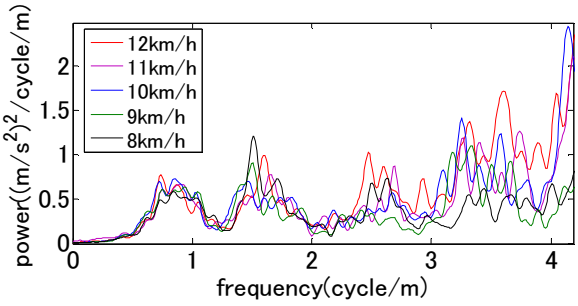

Figure 3.6 Power spectrums at different speed after speed calibration

The effect of tire pressure is then examined. Figure 3.7 shows the power spectrums with various front tire air pressures from 0 to 400 kPa after speed calibration. Though the power spectrums are almost the same below 3 cycle/m, the differences of the power spectrums are larger above 3 cycle/m when the front tire air pressure is higher. In the frequency range below 3 cycle/m, road profile is considered to be the dominant factor of the acceleration responses while tire vibration characteristics is a dominant factor of the response above 3 cycle/m.

The sensitivity of the response to small differences in drive paths is investigated. Figure 3.8 shows the power spectrums of the acceleration responses when the spacing between different drive paths is 20 cm while the course length is about 90 m. The spectrums are calibrated about the speed differences. While the power spectrums are close with each other below 3 cycle/m, the discrepancy is larger as compared to spectrums in Figure 3.6 and Figure 3.7. This result is interpreted that the spectrums below 3 cycle/m slightly differ from each other reflecting the slight difference in road profile.

Three factors affecting the power spectrum of acceleration response, road profile, tire condition, and smartphone holder, were discussed in this section. The smartphone holder affects relatively high frequency components around 14.4 cycle/m (i.e. 40 Hz at 10 km/h). Tire vibration is around 5 cycle/m (i.e. 14 Hz at 10 km/h). Road profile's component below 3 cycle/m are considered to appear in this frequency range. Because repeatability of the signal

below 3 cycle/m is high, double integration of acceleration is expected to represent the road profile in this frequency range.

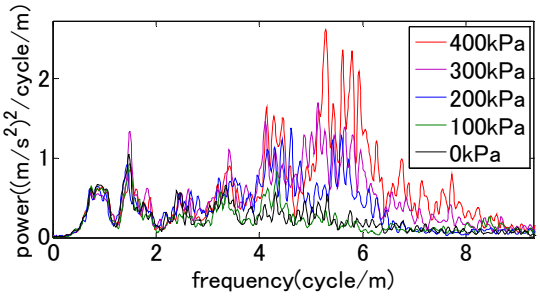

Figure 3.7 Power spectrums with different tire air pressures

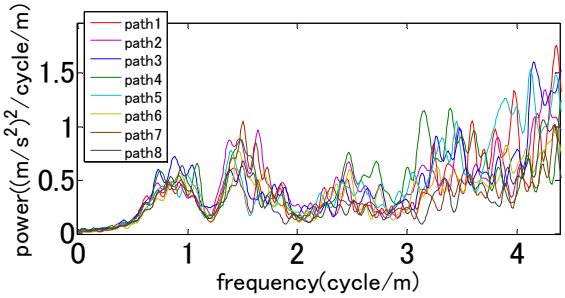

Figure 3.8 Power spectrums at different paths

4. ROAD PROFILE ESTIMATION

4.1. Displacement estimation by double integration of acceleration

If the bicycle is rigid and the inclination angle of the bicycle is small, road displacement *h(t)* should coincide with the smartphone displacement. Bicycle displacement can be estimated by double integration of acceleration *a(t)* as shown in Eq. 4.1.

$$h(t) = \iint_0^t a(t)\,dt \tag{4.1}$$

A 90 meter long straight course on campus is selected as the test course (Figure 4.1 to 4.3). The course contains two speed humps at about 20 m and 80 m from the start point, a manhole at 30 m, and a dome-shaped slope, whose length is about 10 m, at 40 m. The road profile measured by DAM is compared with the displacement estimated from the bicycle acceleration. DAM data is used as the reference to examine profile estimation performance.

Figure 4.1 Picture of the course

Figure 4.2 Speed hump

Figure 4.3 Manhole

The two profile estimation results are different from each other in their magnitudes in Figure 4.4. There is a low frequency noise in estimation data, expected to result from the drift in the smartphone acceleration data. Figure 4.5 shows the profile estimation results after base line correction and high-pass filtering. The cutoff frequency is set as 0.2 Hz (0.07 cycle/m) which is lower than the targeted road profile frequency range; the same high-pass filter is also applied to the DAM data. The two lines are almost the same on the whole, though there are non-negligible differences especially at the second hump.

4.2. Smartphone holder location correction

The smartphone holder location, which is not right above the front tire grounding point, needs to be taken into account (Figure 4.6). The bicycle length *L* is 1.1 m. The horizontal distance *d* between the front tire center and the smartphone holder is 0.15 m. Using the variable *L* and *d*, the smartphone acceleration $a_{smartphone}$ can be

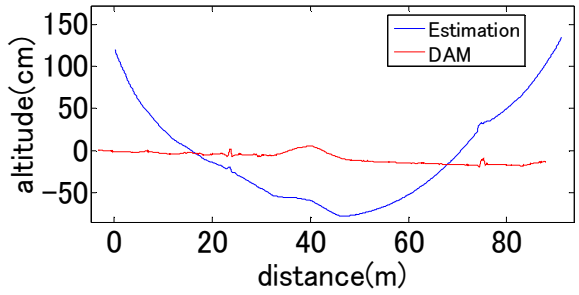

Figure 4.4 Road profile

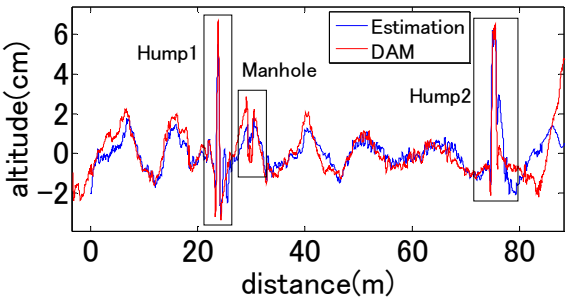

Figure 4.5 Road profile after noise reduction

defined as linear interpolation between the front tire acceleration a_{front} and the rear tire acceleration a_{rear} as stated in Eq. 4.2. a_{rear} is a phase shifted vibration of a_{front}. The phase shift corresponds to the bicycle length L. Assuming harmonic oscillation inputs with phase shift at the front and the rear tire, correction function $k(f)$ (Figure 4.7) from $a_{smartphone}$ to a_{front} is derived as in Eq. 4.3 to 4.6.

$$a_{smartphone} = \frac{(L-d)\times a_{front} + d\times a_{rear}}{L} \tag{4.2}$$

$$a_{front} = k(f)\, a_{smartphone} \tag{4.3}$$

$$k(f) = \frac{L}{\sqrt{A^2+B^2}} e^{-i\frac{B}{A}} \tag{4.4}$$

$$A = L - d + d\cos\frac{2\pi f L}{v} \tag{4.5}$$

$$B = d\sin\frac{2\pi f L}{v} \tag{4.6}$$

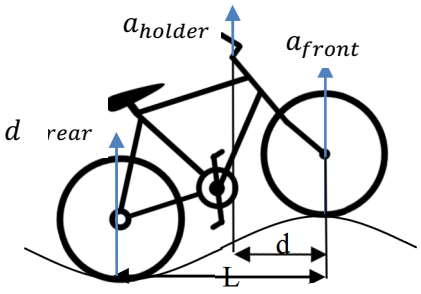

Figure 4.6 Bicycle geometry

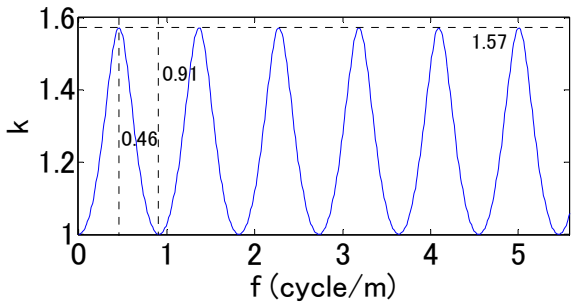

Figure 4.7 Absolute value of correction function $k(f)$

Figure 4.8 is the road profile estimation using the frequency component above 0.2 cycle/m shown in Figure 4.5. The road profile estimations are almost the same in small displacement section, though there are still about 30% difference in the first hump height. Figure 4.9 is the road profile after the smartphone location correction $k(f)$ is applied to the road profile shown in Figure 4.8. The estimated road profile matches the DAM data well even at the two humps; about 10% difference in the first hump height is observed.

Even though frequency components above 3 cycle/m are shown to be strongly affected by the tire pressure, holder natural frequency and other factors, these high frequency components do not contribute to the profile estimation; high frequency components become small through the double integration. Therefore, the frequency components

between 0.2 and 36 cycle/m, which corresponds to the nyquist frequency limit, is utilized in the profile estimation. The frequency range is enough for targeted road surface deformations such as cracks.

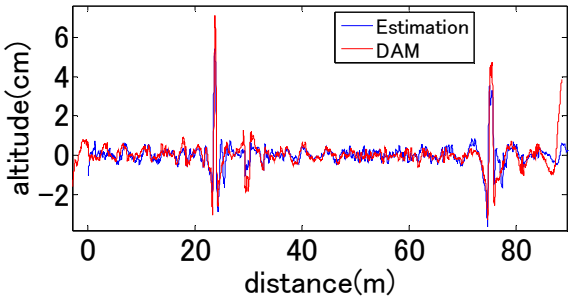

Figure 4.8 Road profile above 0.2 cycle/m

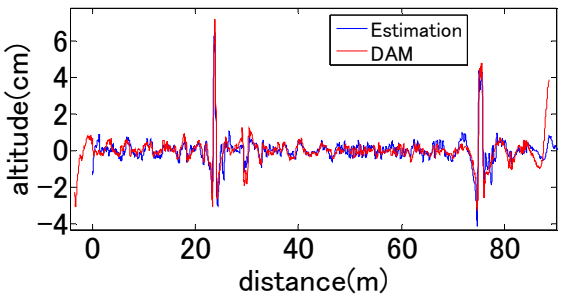

Figure 4.9 Road profile above 0.2 cycle/m after location correction

5. TEST COURSE EXPERIMENT

The Koganei cycling course, a 600 m circular course in Koganei Park, Tokyo, is selected as the test course (Figure 5.1). The course is almost flat while many cracks exist (Figure 5.2). The total number of observed cracks is 91, positioned at 5 to 10 m intervals. Some cracks coincide with large upward displacement; these cracks are lifted up due to the roots of trees nearby. It is important for bicycle lane administrators to detect such locally developed dangerous humps reliably.

Figure 5.1 Picture of Koganei Park

Figure 5.2 crack

Figure 5.3 and 5.4 shows the results of 3 ride tests and DAM measurement. Frequency components above 0.2 cycle/m are utilized. The results of all measurements are almost the same, having only 16 % error in their maximum values (Table 5.1). Figure 5.2 shows the crack at around 337 m point, corresponding to the blue-framed section in Figure 5.3. The crack with large uplift has been detected as a clear peak in calculated road profile.

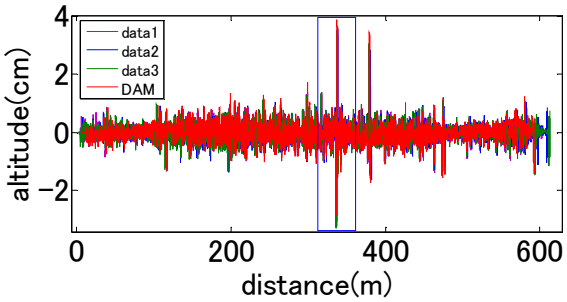

Figure 5.3 Road profile of cycling course

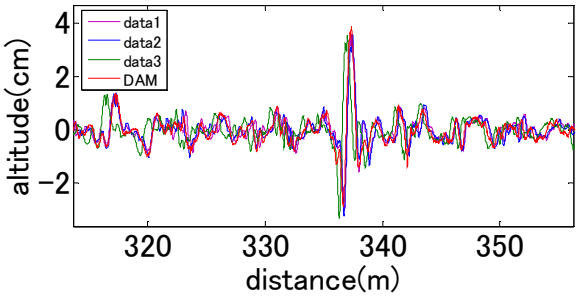

Figure 5.4 Road profile of cycling course at 320 to 350 m

Table 5.1 Maximum peak value

Track #	Peak height (cm)	Error from mean of estimated profile (%)
1	3.37	0
2	3.26	3
3	3.45	3
DAM	3.89	16

6. CONCLUSION

A smartphone based measurement system and the road profile estimation algorithm were developed. The system consists of a commonly used smartphone, bicycle and cyclometer. Using the acceleration data of the smartphone and the cyclometer data, road profiles are estimated.

By conducting free vibration tests and ride tests, bicycle vibration characteristics is examined. The smartphone holder affects relatively high frequency components around 14 cycle/m, while the tire vibration affects frequency components around 5 cycle/m. Frequency components in 0 to 3 cycle/m frequency range is considered to reflect road profile in the same frequency range. The speed calibration equation to calibrate power spectrums at different speed is also proposed.

After smartphone displacement is calculated by double integration of acceleration, the correction function *k(f)* theoretically derived from the relationship among the front tire, rear tire, and smartphone accelerations is applied. Eventually, the road profile components above 0.2 cycle/m are estimated accurately.

The proposed algorithm was validated by an experiment conducted at a bicycle lane course. Estimated road profiles have about 16% error in the maximum values. Also, cracks which coincide with large surface uplifts are clearly detected through the profile estimation.

AKCNOWLEDGEMENT
The author thanks Mr. Ito from NICHIREKI co., LTD for comments that greatly improved the research.

REFERENCES

1. Tokyo Metropolitan Government. Tokyo Prefecture Improvement and Promotion plan for bicycle lanes. http://www.metro.tokyo.jp/INET/KEIKAKU/2012/10/DATA/70mao101.pdf. (2015.6.25 access).
2. Ministry of Land, Infrastructure, Transport and Tourism. Topics about Environment around Bicycle Users. http://www.mlit.go.jp/road/ir/ir-council/bicycle_environ/1pdf/3.pdf. (2015.6.25 access).
3. Sun Top Techno Co., Ltd. Asphalt Tester Road Profiler DAM
4. Y. Kobana, J. Takahashi, I Usami, N Kitsunezaki, Y Tobe, G. Lopez. (2014). Inspection of Road Status by Bicycle Riders: Basic Principle and Preliminary Experiments. Information Processing Society of Japan Technical Reports. 2014-MBL-71(17), 1-7.
5. Y Oshima, T Nagayama, H Salpisoth, H Kawano. (2014). Simple assessment system for road pavement roughness using the responses of a monitor bicycle. Japan Society of Civil Engineers Journal of Structural engineering. Vol.60A pp.475-483.
6. JIP techno Science. HP. http://www.jip-ts.co.jp/. (2015.7.7 access).
7. GARMIN. Property of Edge510J. http://www.garmin.co.jp/products/intosports/edge510j/. (2015.6.25 access).